Eur Spine J (2012) 21 (Suppl 1):S20–S26
DOI 10.1007/s00586-012-2235-x

ORIGINAL ARTICLE

Bioactive electrospun scaffold for annulus fibrosus repair and regeneration

Gianluca Vadalà · Pamela Mozetic · Alberto Rainer · Matteo Centola · Mattia Loppini · Marcella Trombetta · Vincenzo Denaro

Received: 13 February 2012 / Accepted: 19 February 2012 / Published online: 13 March 2012

Abstract
Purpose *Annulus fibrosus* (AF) tissue engineering is gathering increasing interest for the development of strategies to reduce recurrent disc herniation (DH) rate and to increase the effectiveness of intervertebral disc regeneration strategies. This study evaluates the use of a bioactive microfibrous poly(L-lactide) scaffold releasing Transforming Growth Factor (TGF)-β1 (PLLA/TGF) for the repair and regeneration of damaged AF.
Methods The scaffold was synthesized by electrospinning, with a direct incorporation of TGF-β1 into the polymeric solution, and characterized in terms of morphology and drug release profile. Biological evaluation was performed with bovine AF cells (AFCs) that were cultured on the scaffold up to 3 weeks to quantitatively assess glycosaminoglycans and total collagen production, using bare electrospun PLLA as a control. Histological evaluation was performed to determine the thickness of the deposited neo-ECM.
Results Results demonstrated that AFCs cultured on PLLA/TGF deposited a significantly greater amount of glycosaminoglycans and total collagen than the control, with higher neo-ECM thickness.
Conclusions PLLA/TGF scaffold induced an anabolic stimulus on AFCs, mimicking the ECM three-dimensional environment of AF tissue. This bioactive scaffold showed encouraging results that allow envisaging an application for AF tissue engineering strategies and AF repair after discectomy for the prevention of recurrent DH.

Keywords *Annulus fibrosus* · Bioactive scaffold · Intervertebral disc · Tissue engineering · Electrospinning · Drug release · Recurrent disc herniation · TGF-β1

G. Vadalà (✉) · M. Loppini · V. Denaro
Department of Orthopaedics and Trauma Surgery, CIR—Center for Integrated Research, Università Campus Bio-Medico di Roma, via Álvaro del Portillo 200, 00128 Rome, Italy
e-mail: g.vadala@gmail.com

P. Mozetic · A. Rainer · M. Centola · M. Trombetta
Tissue Engineering Laboratory, CIR—Center for Integrated Research, Università Campus Bio-Medico di Roma, via Álvaro del Portillo 21, Rome, Italy

Introduction

Lumbar disc herniation (DH) has a lifetime prevalence of 1–3% in Western Countries [1]. Although standard discectomy is an effective treatment in relieving neurological symptoms, it deeply changes the biomechanics of the spinal functional unit. Indeed, it causes significant nucleus pulposus (NP) loss and intervertebral disc (IVD) height reduction. These modifications lead to functional changes of the disc that limit its role as a shock absorber [2]. As a consequence, degenerative spondylosis occurs in association with the reappearance of low back pain after surgery. Kambin et al. [3] reported a 39% rate of degenerative post-discectomy spondylosis. Another complication after discectomy is the high rate of DH recurrence, affecting up to 12.5% of patients [4], with a re-surgery rate ranging from 3 to 15% [5, 6].

Exciting advances in the field of tissue engineering have allowed spine researchers to begin developing novel therapeutic approaches in an attempt to intervene in and modulate the course of IVD degeneration by repairing, replacing or regenerating the herniated or degenerated NP [7–10]. However, these strategies are ineffective without a functional annulus fibrosus (AF) able to withstand the physiological intradiscal pressure. Therefore, new strategies to augment, repair, or regenerate AF are strongly needed with

the attempt to both reduce recurrent DH rate and increase the effectiveness of NP regenerative strategies.

Tissue engineering combines cells and scaffolds with features ranging from micro- to nanoscale and high porosity, resembling the natural extracellular matrix (ECM) arrangement, to produce specific tissues. Among the available technologies for scaffolds fabrication, electrospinning is gaining growing interest for its ability to produce micro- and nanofibrous structures, which represent an ideal microenvironment for cell adhesion, proliferation, and differentiation [11]. Moreover, electrospinning process allows scaffold functionalization, by encapsulation of different bioactive agents, which can modulate the activity of seeded cells. A number of molecules can be delivered, including antibiotics, anticancer drugs, and proteins [12, 13]. Bioactive nanoparticles dispersed in electrospun microfibers have demonstrated a capacity to modulate the differentiation of human mesenchymal stem cells (hMSCs) [11].

AF tissue engineering approaches have evaluated AF cells seeded in several types of 3D hydrogels or scaffolds [7, 14–18]. These studies have demonstrated that AF cells proliferate in 3D culture and synthesize ECM, reconstituting the histological structure of native tissue. Since degeneration of IVD tissue components reflects an imbalance in the normal anabolic and catabolic functions of IVD cells, regeneration of AF tissue might be mediated by enhancing anabolic signals. Researchers have demonstrated that bioactive agents, such as Transforming Growth Factor Beta 1 (TGF-β1), are able to increase AF cell proliferation and ECM production, stimulating secretion and assembly of glycosaminoglycans and collagen [19, 20].

In this study, we propose the use of a bioactive electrospun scaffold releasing TGF-β1 for AF repair and regeneration. The objective is to assess viability of bovine AF cells onto randomly oriented electrospun poly(L-lactide) (PLLA) fibers functionalized with TGF-β1 and to evaluate growth factor release over time and ECM production by bovine AF cells under that stimulus.

Methods

Scaffold preparation and characterization

TGF-β1-functionalized PLLA scaffolds (PLLA/TGF) were prepared by electrospinning, starting from 13% w/w PLLA (Sigma, MO, USA) solution in dichloromethane (Sigma). TGF-β1 (Sigma) was added to the polymer solution at a concentration of 20 ng per gram of PLLA. An electrospinning equipment was used (DynaSpin, Biomatica, Italy); the solution was fed at a rate of 1.5 mL/h through a 28G needle kept at a high potential (15 kV) versus an earthed collector placed at a distance of 15 cm. Bare PLLA scaffolds (without TGF-β1 addition, PLLA/Ctrl) were obtained in the same experimental conditions to be used as a control. Microstructure of membranes was evaluated by Field Emission Scanning Electron Microscopy (FE-SEM) (Supra 1535; LEO Electron Microscopy, UK). Drug release from the scaffolds was also evaluated. PLLA/TGF scaffold were placed in phosphate buffered saline (PBS) and incubated at 37°C. Supernatant were timely collected and TGF-β1 concentration was quantified by means of an ELISA test (hTGF-β1 Instant ELISA, Bender MedSystems, CA, USA), in accordance with the manufacturer's instructions. Absorbance was read on a microplate reader (Tecan, Männedorf, CH) at 450 nm with correction at 620 nm.

Cell isolation

A bovine tail was obtained from a local abattoir. Tail discs were removed from the *vertebrae* under sterile conditions and dissected into NP and AF. AF tissue was digested following an already established procedure by 0.2% pronase digestion (Calbiochem, CA, USA) for 90 min and subsequent 0.01% collagenase type 2 (Worthington, UK) digestion overnight. The digest was filtered and AF cells cultured with F-12 with 10% fetal bovine serum (FBS; Gibco), 1% penicillin/streptomycin (P/S; Gibco), and 1% glutamine (Gibco) at 37°C in a 5% CO_2 humidified atmosphere and expanded in monolayer up to Passage 2.

Cytotoxicity assays

Bovine AF cells (AFCs) were plated in a 96-well plate (BD Falcon, San Jose, CA, USA) at a density of 1×10^4 cells/well and cultured in growing medium for 24 h. PLLA/TGF or PLLA/Ctrl scaffolds were then selectively added to each well. Scaffold cytotoxicity was assessed at 4, 8, and 24 h using Vybrant Cytotoxicity Assay Kit (Molecular Probes, Invitrogen) following manufacturer's instructions. Plate was read on a fluorescence microplate reader (Tecan, excitation 535 nm, emission 595 nm). Data were normalized against cell lysates.

Seeding and culture AF cells on the scaffolds

PLLA/TGF and PLLA/Ctrl scaffolds were punched out to disks 6 mm in diameter, UV sterilized (20 min), and placed into a 96-well low-adhesion plate (Ultra Low Attachment Plate, Corning, USA). AFCs were seeded at a density of 5×10^5 cell/cm^2 on PLLA/TGF or PLLA/Ctrl scaffolds using a static seeding technique. Constructs were cultured for 21 days in standard conditions and medium changes. Additionally, monolayer cultures of AFC on conventional plasticware were performed and exposed to

the elution products of PLLA/TGF and PLLA/Ctrl scaffolds. Cells were seeded at the density of 1.8×10^5 cell/cm^2 into a 96-well plate. After 6 h, PLLA/TGF and PLLA/Ctrl scaffolds were selectively added to each well and cells were cultured for 21 days (according to the previous protocol).

DNA content

Total DNA of samples was extracted with TRIzol reagent (Invitrogen) according to the manufacturer's protocol. DNA of each sample was measured by Quant-iT dsDNA HS assay (Invitrogen) on a Qubit Fluorometer (Invitrogen) at 485/530 nm (excitation/emission), following the manufacturer's instructions.

Glycosaminoglycan content

The glycosaminoglycans (GAG) were extracted from the bAFC cultures by adding 200 μL of papain digestion buffer (50 mM phosphate buffer, 5 mM EDTA, 5 mM cysteine·HCl and 0.25 mg/mL papain) to each well, followed by incubation at 60°C overnight. The standard curve was from chondroitin-6-sulfate (Sigma). The papain buffer containing the proteoglycans was collected and 1,9-dimethyl-methylene blue (DMMB) added. The total GAG content was measured quantitatively using an optical density plate reader (at 540 and 595 nm, Tecan). Results were normalized by DNA content.

Collagen content

Samples were fixed in absolute ethanol for 3 min, washed and stained with Sirius Red staining solution (0.1% Sirius Red in sat. aqueous picric acid) at 37°C for 18 h. After incubation, excess staining was removed by washing, and a 0.1 M NaOH solution in absolute methanol was added into each well. Final solution from each sample was read on a plate reader at 490 nm (Tecan). Results were normalized by DNA content.

Histology evaluation

Cell/scaffold constructs were fixed in PFA, embedded in OCT compound (Fisher Scientific, Canada), snap frozen, and cryosectioned with a thickness of 7 μm. Sections were stained with hematoxylin/eosin (Sigma) and analyzed qualitatively under a light microscope (Olympus BX51, Japan); 10 images at 40× magnification were acquired every 600 μm for the overall length of the membrane to evaluate the thickness of the neo-ECM synthesized. Measurements were taken in three different points of the constructs on each slide (ImageJ ver. 1.44, NIH, USA).

Statistical analysis

Experiments were conducted in quintuplicate at the same experimental conditions. Data were processed using SPSS (Version 13.0). Student's *t* test was performed to compare experimental and control groups. Significance was at the 0.05 level. Data are presented as mean ± standard deviation.

Results

Scaffolds characterizations

Electrospun scaffolds consisted of a non-woven porous mesh with randomly oriented fibers, but significant differences in fibers morphology could be found between the two groups (Fig. 1). PLLA/Ctrl fibers were micron-sized (average diameter 1.5 ± 0.9 μm) and showed an intrinsic porosity, with elongated pores sized around 100 nm. PLLA/TGF scaffolds, instead, showed smaller diameter (average diameter 620 ± 170 nm) fibers.

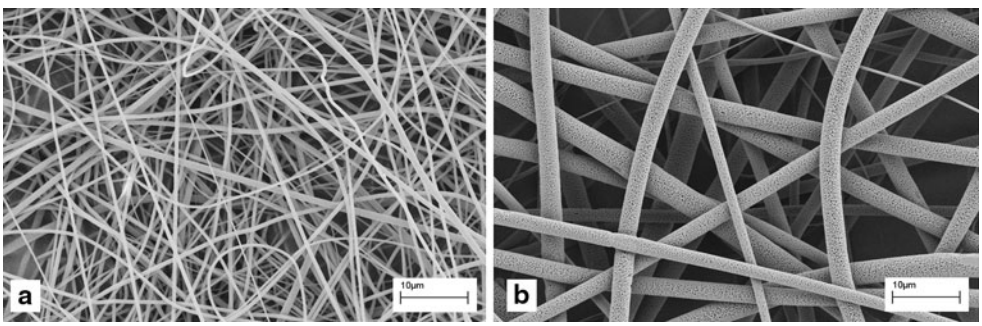

Fig. 1 Representative images of the PLLA/TGF **(a)** and PLLA/Ctrl **(b)** scaffold observed with the Field Emission Scanning Electron Microscopy. Both scaffolds consist of a non-woven porous fibrous mesh, but significant differences can be found in fibermorphology. *Scale bar* 10 μm

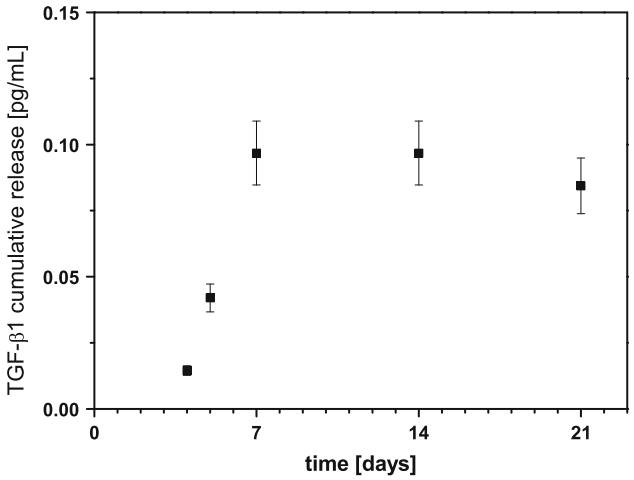

Fig. 2 TGF-β1 release over time from PLLA/TGF scaffold

Detectable concentrations of TGF-β1 assessed by ELISA were measured only after 4 days, and cumulative release reached a *plateau* after day 7 (Fig. 2).

Cell viability

The evaluation of the release of the cytosolic enzyme G6PD from damaged bovine AFCs into the surrounding medium after cell exposure to PLLA/TGF and PLLA/Ctrl scaffolds showed cell viability higher than 95% at each time point (Fig. 3).

ECM content

Results of GAG quantification are shown in Fig. 4a, normalized with respect to DNA content ($\mu g_{GAG}/\mu g_{DNA}$).

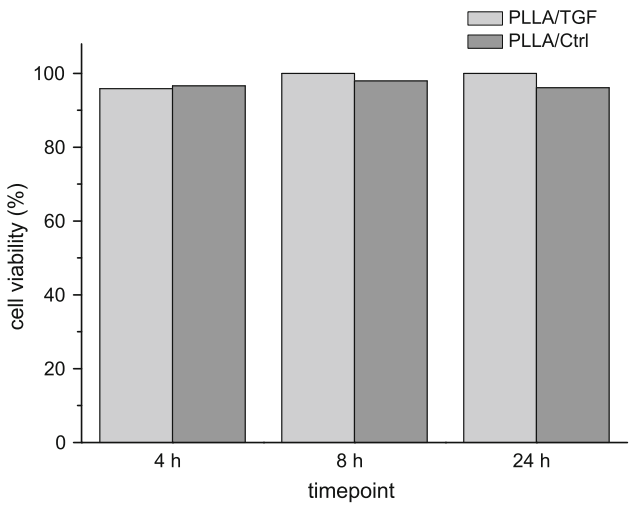

Fig. 3 Cell viability determined as the release of the cytosolic enzyme glucose-6-phosphate dehydrogenase from damaged cells into the surrounding medium by bovine AFCs exposed to PLLA/TGF and PLLA/Ctrl scaffolds for 4, 8, and 24 h

GAG content in PLLA/TGF constructs was significantly higher than the one reported for PLLA/Ctrl (2.68 ± 0.23 vs. 1.4 ± 0.24 $\mu g_{GAG}/\mu g_{DNA}$, $p < 0.05$).

Similar trend was reported for 2D control cultures of AFCs performed in the presence of the scaffolds. GAG content was significantly higher for AFCs exposed to PLLA/TGF compared with PLLA/Ctrl (Fig. 4b).

A significantly higher level of total collagen production was observed in PLLA/TGF constructs compared with PLLA/Ctrl ($p < 0.05$) expressed in terms of absorbance and normalized versus DNA content (Fig. 5a). Similarly, in 2D control cultures, total collagen production was significantly higher for AFCs culture exposed to PLLA/TGF with respect to PLLA/Ctrl control ($p < 0.05$) (Fig. 5b).

Histological analysis

H&E staining showed the presence of neo-ECM produced on the both sides of the scaffolds (Fig. 6a, b). Qualitative analysis of the samples shows that AFCs produced a higher amount of neo-ECM on PLLA/TFG constructs with respect to PLLA/Ctrl. Thickness of neo-synthesized ECM on the scaffold surface was measured by image analysis. ECM thickness on PLLA/Ctrl constructs was 18.72 ± 7.26 μm, while its value on PLLA/TGF constructs was 48.90 ± 16.05 μm (Fig. 5c), representing a significant difference ($p < 0.05$).

Discussion

To date, several scaffolds have been described targeting AF tissue replacement. Nerurkar et al. [18] analyzed an electrospun aligned nanofibrous PCL scaffold using bovine AFCs in vitro. The authors showed that AFCs oriented along the fibers and exhibited some physiological behavior of AF *lamellae* in the loaded construct. Furthermore, Gruber et al. [16] showed that culture of human AFCs on electrospun polyamide nanofibers is permissive for secretion and assembly ECM components. Recently, a new study of Nerurkar et al. [17] described a nanofibrous laminate that replicated the micro-architecture and tensile properties of AF. Furthermore, those authors showed the role of inter-lamellar ECM in reinforcing the tensile response of biologic laminates. Given the importance of the quantity and quality of ECM production in AF tissue engineering, the use of scaffolds providing biomolecular signals for AF regeneration could be beneficial. In the present study, we aim to demonstrate the role played by TGF-β1 released by an electrospun scaffold in the production of ECM.

Morphological characterization of the scaffolds performed by FE-SEM revealed substantial changes in fiber

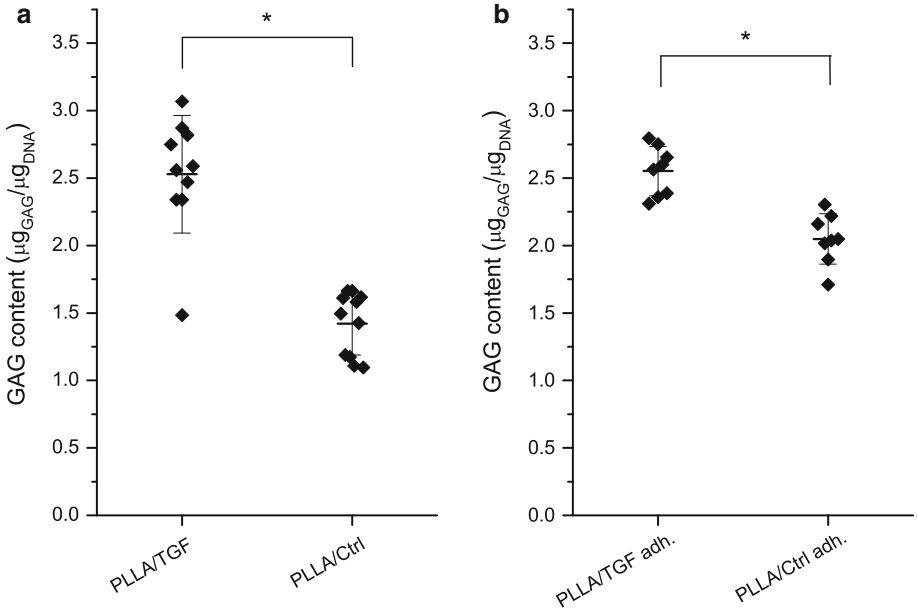

Fig. 4 Glycosaminoglycan determination by DMMB assay after 3 weeks culturing. **a** AFCs cultured on PLLA/TGF and PLLA/Ctrl scaffolds. **b** AFCs cultured in adhesion on conventional plasticware in the presence of PLLA/TGF and PLLA/Ctrl scaffolds. *Asterisk* denotes significance at the 0.05 level

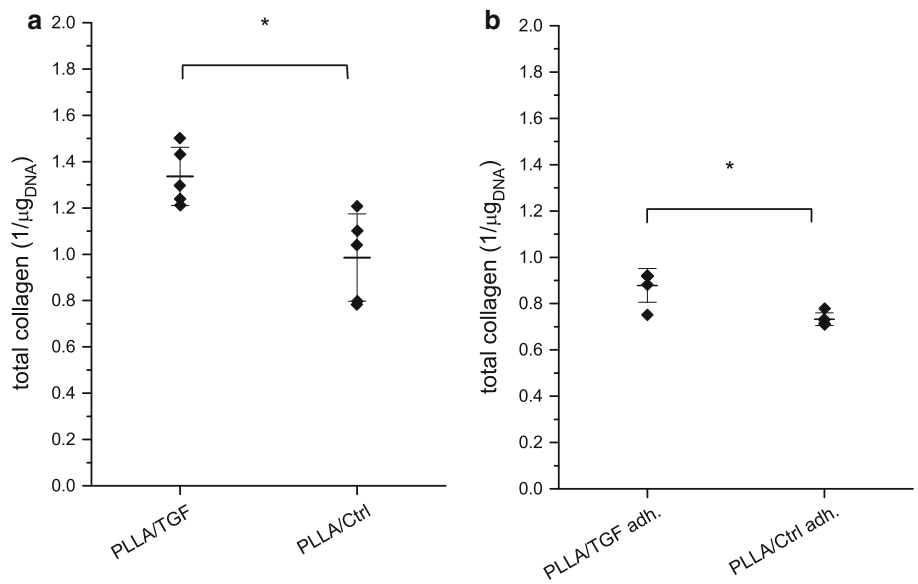

Fig. 5 Total collagen determination by Sirius Red assay after 3 weeks culturing. **a** AFCs cultured on PLLA/TGF and PLLA/Ctrl scaffolds. **b** AFCs cultured in adhesion on conventional plasticware in the presence of PLLA/TGF and PLLA/Ctrl scaffolds. *Asterisk* denotes significance at the 0.05 level

Fig. 6 Representative histological sections of PLLA/TGF (**a**) and PLLA/Ctrl (**b**) after 3 weeks' culturing with AFCs (hematoxylin/eosin staining). *Scale bar* 100 µm. The neo-ECM in (**a**) appears more abundant than in (**b**). **c** Thickness of the neo-ECM layer on PLLA/TGF and PLLA/Ctrl constructs as determined by image analysis on histological sections. *Asterisk* denotes significance at the 0.05 level

morphology between PLLA/TGF and PLLA/Ctrl. In functionalized scaffolds, addition of the drug modified solution parameters (e.g. viscosity and conductivity), affecting the electrospinning process, and leading to thinner fibers. Additionally, PLLA/Ctrl fibers were characterized by an intrinsic porosity, attributable to a phase separation process during solvent evaporation [21], which was less evidenced in PLLA/TGF samples. Results of the drug release assay performed on PLLA/TGF scaffold showed that eluted drug reached a detectable concentration on day 5, and cumulative release profile reached a plateau on day 7. The slightly diminishing value reported at day 21 could be ascribed to protein denaturation.

AFCs demonstrated good viability when cultured on either electrospun PLLA/TGF or PLLA/Ctrl scaffolds, thanks to the micro-architecture of fibers, able to mimic the ECM morphology and provide a suitable substrate for cell adhesion. However, cells seeded on functionalized scaffolds produced a higher amount of GAG and collagen, confirming the anabolic effect of TGF-β1 in terms of ECM synthesis. Histological analysis showed that the neo-synthesized ECM layer on PLLA/TGF scaffolds was thicker than the control, as indicated by image analysis on histological sections.

It is well known that surface topography, stiffness, and scaffold porosity play a critical role in cell behavior and tissue growth [22]. To evaluate the potential role of differences in scaffold morphology (PLLA/TGF vs. PLLA/Ctrl) on AFC anabolism, cells were also cultured in monolayer and exposed to the scaffolds, without any direct contact. We observed a significant increase in both GAG and collagen content on cells exposed to PLLA/TGF compared with PLLA/Ctrl. Such results confirm that the anabolic effect on AFCs has to be attributed to the release of TGF-β1, rather than to slight differences in scaffold microstructure.

In a clinical setting, such a scaffold might be used after discectomy to cork the hole in AF left after DH and surgical procedure. The scaffold might either be sutured or fixed with fibrin glue or other biological glue materials. This bioactive scaffold might also be associated with NP tissue engineering strategies for the treatment of IVD degeneration. In fact, NP replacement therapies could be destined to fail, when used without specific approaches addressed to repair damaged AF, since a regenerated NP must support the physiological intradiscal pressure thanks to a competent AF. Moreover, it has been recently reported that cell therapeutic approaches for IVD still suffer of cell-transfer effectiveness such as cell leakage after intradiscal injection [23, 24]. Therefore, AF sealing and regeneration technologies appear to be important fields of investigation in the way to develop a stem cell-based approach for IDD treatment.

While the use of AFCs in an in vitro environment allows studying the effect of the scaffold on cell activity, the use of AFCs for IVD tissue engineering may be questioned, since they are difficult to harvest, and require multi-step surgical procedures. Moreover, extensive in vitro culturing of AFCs may lead to cell dedifferentiation and cell senescence [25]. An attractive alternative for AF tissue engineering would be the use of hMSCs. However, while hMSCs can differentiate in NP cells [8, 10, 26], differentiation into AFCs has not been demonstrated yet. Sobajima et al. [27] showed that, 24 weeks after MSCs transplantation in normal rabbit disc, MSCs were localized in the inner AF, where they exhibited an apparent change in morphology to a spindle shape more similar to native AFCs. Indeed, further studies are needed to evaluate the MSC regenerative capacity for AF repair. However, the association with progenitor cells opens new perspectives in the development of tissue-engineered constructs able to regenerate a tissue deficit in a degenerated or damaged AF.

Conclusion

This study demonstrated that a poly(L-lactide) electrospun scaffold functionalized with TGF-β1 was able to provide sustained release of the growth factor and to induce an anabolic *stimulus* on AFCs, while mimicking the ECM three-dimensional environment of the AF tissue. These positive results allow envisaging a potential application of the developed scaffold in tissue engineering strategies for the treatment of degenerated IVD, including repair of damaged AF and prevention of recurrent DH.

Acknowledgments The authors would like to gratefully acknowledge Dr. Franca Abbruzzese for her help in the cell viability analyses. The support of the Stem Cells Research Group of the Italian Society of Spine Surgery (GIS) and the Research Grant (PRIN2009) of the Italian Minister of Instruction, University and Research (MIUR) are gratefully acknowledged.

Conflict of interest None.

References

1. Weber H (1994) The natural history of disc herniation and the influence of intervention. Spine (Phila Pa 1976) 19:2234–2238 (discussion 2233)
2. Moore AJ, Chilton JD, Uttley D (1994) Long-term results of microlumbar discectomy. Br J Neurosurg 8:319–326
3. Kambin P, Cohen LF, Brooks M, Schaffer JL (1995) Development of degenerative spondylosis of the lumbar spine after partial discectomy. Comparison of laminotomy, discectomy, and posterolateral discectomy. Spine (Phila Pa 1976) 20:599–607
4. Yorimitsu E, Chiba K, Toyama Y, Hirabayashi K (2001) Long-term outcomes of standard discectomy for lumbar disc herniation:

a follow-up study of more than 10 years. Spine (Phila Pa 1976) 26:652–657
5. Suk KS, Lee HM, Moon SH, Kim NH (2001) Recurrent lumbar disc herniation: results of operative management. Spine (Phila Pa 1976) 26:672–676
6. Vucetic N, de Bri E, Svensson O (1997) Clinical history in lumbar disc herniation. A prospective study in 160 patients. Acta Orthop Scand 68:116–120
7. Alini M, Li W, Markovic P, Aebi M, Spiro RC, Roughley PJ (2003) The potential and limitations of a cell-seeded collagen/hyaluronan scaffold to engineer an intervertebral disc-like matrix. Spine (Phila Pa 1976) 28:446–454 discussion 453
8. Vadala G, Studer RK, Sowa G, Spiezia F, Iucu C, Denaro V, Gilbertson LG, Kang JD (2008) Coculture of bone marrow mesenchymal stem cells and nucleus pulposus cells modulate gene expression profile without cell fusion. Spine (Phila Pa 1976) 33:870–876
9. Hubert MG, Vadala G, Sowa G, Studer RK, Kang JD (2008) Gene therapy for the treatment of degenerative disk disease. J Am Acad Orthop Surg 6:312–319
10. Vadala G, Sobajima S, Lee JY, Huard J, Denaro V, Kang JD, Gilbertson LG (2008) In vitro interaction between muscle-derived stem cells and nucleus pulposus cells. Spine J 8:804–809
11. Spadaccio C, Rainer A, Trombetta M, Vadala G, Chello M, Covino E, Denaro V, Toyoda Y, Genovese JA (2009) Poly-L-lactic acid/hydroxyapatite electrospun nanocomposites induce chondrogenic differentiation of human MSC. Ann Biomed Eng 37:1376–1389
12. Bolgen N, Vargel I, Korkusuz P, Menceloglu YZ, Piskin E (2007) In vivo performance of antibiotic embedded electrospun PCL membranes for prevention of abdominal adhesions. J Biomed Mater Res B Appl Biomater 81:530–543
13. Xu X, Chen X, Xu X, Lu T, Wang X, Yang L, Jing X (2006) BCNU-loaded PEG-PLLA ultrafine fibers and their in vitro antitumor activity against Glioma C6 cells. J Control Release 114:307–316
14. Shao X, Hunter CJ (2007) Developing an alginate/chitosan hybrid fiber scaffold for annulus fibrosus cells. J Biomed Mater Res A 82:701–710
15. Mizuno H, Roy AK, Vacanti CA, Kojima K, Ueda M, Bonassar LJ (2004) Tissue-engineered composites of anulus fibrosus and nucleus pulposus for intervertebral disc replacement. Spine (Phila Pa 1976) 29:1290–1297 discussion 1297–1298
16. Gruber HE, Hoelscher G, Ingram JA, Hanley EN Jr (2009) Culture of human anulus fibrosus cells on polyamide nanofibers: extracellular matrix production. Spine (Phila Pa 1976) 34:4–9. doi:10.1097/BRS.0b013e31818f8c02
17. Nerurkar NL, Baker BM, Sen S, Wible EE, Elliott DM, Mauck RL (2009) Nanofibrous biologic laminates replicate the form and function of the annulus fibrosus. Nat Mater 8:986–992
18. Nerurkar NL, Elliott DM, Mauck RL (2007) Mechanics of oriented electrospun nanofibrous scaffolds for annulus fibrosus tissue engineering. J Orthop Res 25:1018–1028
19. Moon SH, Nishida K, Gilbertson LG, Lee HM, Kim H, Hall RA, Robbins PD, Kang JD (2008) Biologic response of human intervertebral disc cells to gene therapy cocktail. Spine (Phila Pa 1976) 33:1850–1855. doi:10.1097/BRS.0b013e31817e1cd7
20. Thompson JP, Oegema TR Jr, Bradford DS (1991) Stimulation of mature canine intervertebral disc by growth factors. Spine (Phila Pa 1976) 16:253–260
21. Bognitzki M, Czado W, Frese T, Schaper A, Hellwig M, Steinhart M, Greiner A, Wendorff JH (2001) Nanostructured fibers via electrospinning. Adv Mater 13:70–72
22. Dalby MJ, Gadegaard N, Tare R, Andar A, Riehle MO, Herzyk P, Wilkinson CD, Oreffo RO (2007) The control of human mesenchymal cell differentiation using nanoscale symmetry and disorder. Nat Mater 6:997–1003
23. Omlor GW, Bertram H, Kleinschmidt K, Fischer J, Brohm K, Guehring T, Anton M, Richter W (2010) Methods to monitor distribution and metabolic activity of mesenchymal stem cells following in vivo injection into nucleotomized porcine intervertebral discs. Eur Spine J 19:601–612
24. Vadala G, Sowa G, Hubert M, Gilbertson LG, Denaro V, Kang JD (2011) Mesenchymal stem cells injection in degenerated intervertebral disc: cell leakage may induce osteophyte formation. J Tissue Eng Regen Med. doi:10.1002/term.433
25. Maldonado BA, Oegema TR Jr (1992) Initial characterization of the metabolism of intervertebral disc cells encapsulated in microspheres. J Orthop Res 10:677–690
26. Sakai D, Mochida J, Iwashina T, Watanabe T, Nakai T, Ando K, Hotta T (2005) Differentiation of mesenchymal stem cells transplanted to a rabbit degenerative disc model: potential and limitations for stem cell therapy in disc regeneration. Spine 30:2379–2387
27. Sobajima S, Vadala G, Shimer A, Kim JS, Gilbertson LG, Kang JD (2008) Feasibility of a stem cell therapy for intervertebral disc degeneration. Spine J 8:888–896